External Partial Discharge Analysis in Design Process of Electrical Space Components

Arentsen , Martin Trolle; Bak, Claus Leth; Silva, Filipe Miguel Faria da; Lorenzen, Søren

Published in:
Proceedings of 2019 European Space Power Conference (ESPC)

DOI (link to publication from Publisher):
10.1109/ESPC.2019.8932001

Publication date:
2019

Document Version
Accepted author manuscript, peer reviewed version

Partial Discharges of High Frequency Transformer for Space Application in Near Vacuum

M. T. Arentsen[1,3,*], C. L. Bak[1], F. F. da Silva[1] and S. Lorenzen[3]

1Aalborg University, Pontoppidanstræde 111, 9220 Aalborg Ø, Denmark
[2]Flux A/S, Industrivangen 5, 4550 Asnæs, Denmark
[3]DEIF A/S, Frisenborgvej 33, 7800 Skive, Denmark

*Email: mtarentsen@yahoo.com

Abstract. This paper presents partial discharge measurements and a model-based investigation for corona activity on a prototype of a high frequency transformer from Flux A/S, designed to operate on a space travelling vessel. Previous iterations of the prototypes failed external partial discharge tests, and the environment that the transformer was designed to be installed and tested in, was suspected to cause the partial discharge to onset. In normal operation on the space vessel (and during the required design-tests), the transformer has its terminals exposed to the surrounding atmosphere, whose pressure varies from standard atmospheric pressure to near vacuum conditions during the launch of the space vessel. The most critical condition for external partial dielectric breakdown will be encountered under its intended operation, similar to the knee point in the Paschen curve. The conditions at this point yields the largest stresses on the dielectric, in this case the surrounding atmosphere of the transformer. A predictive method for evaluation of corona activity onset is therefore included. This is done based on calculation of the effective ionization coefficient along the critical electrical field line, $\overline{\alpha}$, obtained by Finite Element Method (FEM) models and is evaluated for a given set of pressure values to emulate the intended operating conditions of the transformer. $\overline{\alpha}$ itself is a function of the electrical field strength along the critical line, as well as the relative air density. The FEM models of the transformer were therefore designed to calculate the electrical field strength distribution around the transformer, and to locate the critical field line. It was found that 2D models yielded a satisfactory accuracy for the intention of the simulation, and that 3D models would only yield a slightly improved accuracy for a substantially increased computational burden.

For the partial discharge measurements, the test voltage was 1 kV at 50 Hz, and the geometry of the transformer and distances to objects in proximity to the transformer will remain constant, leading to the electrical field strength distribution also being constant. The only varying parameter which is affecting $\overline{\alpha}$ is the variation of the atmospheric pressure. The corona activity onset condition is evaluated by evaluating the integral value of $\overline{\alpha}$ over its region that yields a net positive ionization and compare this value with the criteria for the Townsend mechanism. The simulated pressure range includes only values that are realizable with the available equipment in the HV-laboratory of Aalborg University, which is 1.0 to 0.2 bars of absolute pressure. This is done with the intention to compare the predictive method for corona onset with actual partial discharge measurements. The PD measurements showed that no external partial discharge activity was present for the given experimental conditions and pressure range, and the new design of the transformer prototype was therefore improved.

Keywords: Corona, Space Application, Partial Discharge Measurement, High Voltage Measurement Techniques, FEM Simulation.

1 Introduction

An experimental- and model-based investigating of external partial discharge activity on a prototype of a high frequency transformer for space applications will be presented in this paper. The transformer prototype is designed for an ion-motor on a space vessel by Flux A/S, and testing of the first iterations of the prototype showed unsatisfactory levels of PD-activity according to the governing standard ECSS (European Cooperation of Space Standardization). The measurements were performed at various absolute atmospheric pressure levels to emulate the intended operational environment of the transformer during launch into space of the space vessel.

The primary goal was to investigate the prototype by experimental means, while a method for model-based investigation was highly desired as well, since none was available to Flux A/S in their design process. Both investigations were conducted and are shown in this paper.

The model-based investigation was done by designing a Finite Element Method (FEM) model of the transformer, in order to calculate the electrical field distribution as well as locating the critical field line. Conventional corona onset evaluation was not used, which usually is done by assessing the field strength at the critical point. Instead, corona onset evaluation will be done based on calculation of the effective ionization along the critical field line, which is a function of the applied voltage, the geometry of the Device Under Test (DUT) and surrounding atmosphere and its relative density. This modelling- and corona onset evaluation approach is described in more detail in the State-of-the-Art section, and the intention of the model-based investigation is to serve as a rough estimation tool for evaluating the expectancy of corona being present on the test object for a given set of test conditions

2 PD Measurement Setup & Results

The PD-measurement test performed on the first iterations of the prototypes were lacking useful details, since the equipment available to Flux A/S had no Phase-Resolved-Partial-Discharge (PRPD) measurement capability – however, a corona glow was observed during their test.

In accordance with IEC 60270 “High-Voltage Test Techniques – Partial Discharge Measurements” [1], a PD-measurement setup with PRPD measurement capabilities was designed to test the prototype for any PD activity, and the circuit can be seen in Figure 1.

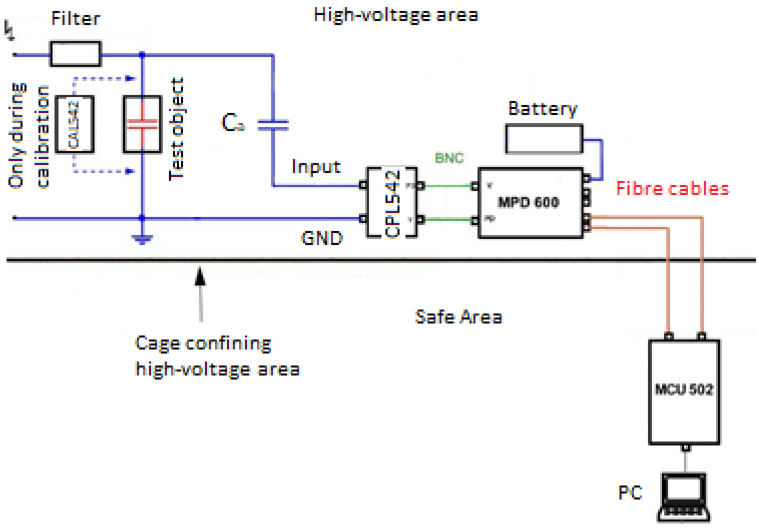

Fig. 1. PD-Measurement circuit, consisting of Calibration Unit CAL 542, Coupling quadripole CPL 542, PD Measurement unit MPD 600 and the ADC MCU 502 [2].

The DUT being the transformer prototype, is situated in the vacuum chamber, seen in Figure 2, which is used to vary the atmospheric pressure to emulate the ambient conditions during assent of the space vessel. According to ECSS [3], the PD-Measurement test must be performed in as close to intended operating conditions as possible, rendering the atmospheric pressure variation a necessity.

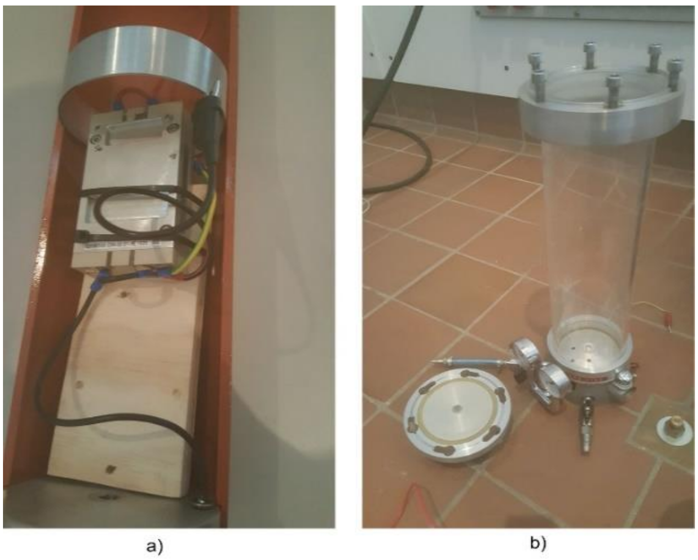

Fig. 2. a) Transformer prototype in suspension chamber. b) Vacuum chamber, which suspension chamber is inserted into.

Conducting the PD-Measurements according to ECSS procedure and requirements, conforming with IEC 60270, and repeating for pressure levels from 1.0 bar to 0.2 bars of absolute pressure (Maximum capability of pressure vessel and pump) to emulate the intended operating environment during assent yielded PD-Measurements seen in Figure 3.

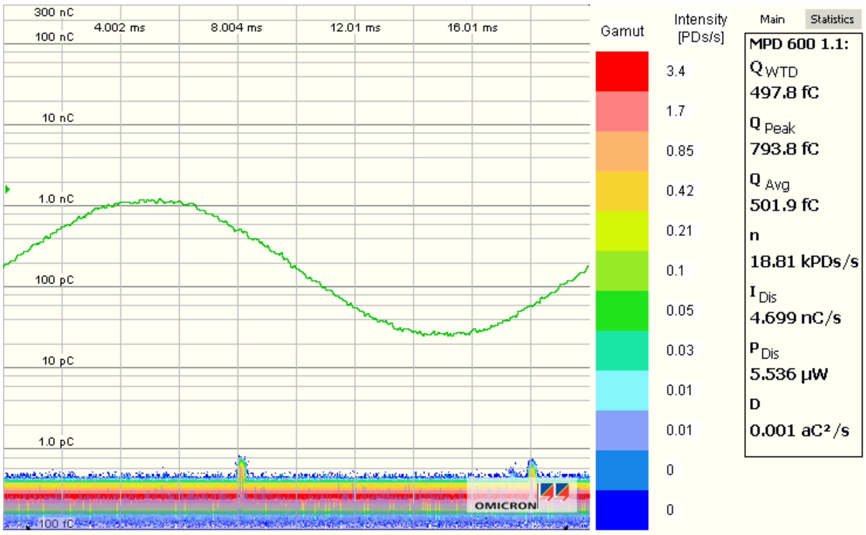

Fig. 3. PD-Measurement of transformer prototype at 0.2 Bar over duration of 10 minutes. Apparent activity hotspots at ~ -45° from zero-crossing.

Looking at Figure 3, it seems like PD activity was present between the peak and zero-crossing of the applied voltage waveform. It was discovered that this was caused by the measurement equipment picking up noise levels of 0.8 pC phase shifted 180° of each other, and wrongly getting corelated to a fixed spot of the applied voltage. This was discovered by monitoring the PD-measurements while no voltage was applied, where these two peaks drifted along the phase-axis of Figure 3, until voltage was applied gradually, and the peaks was wrongly corelated to these particular phase positions.

Figure 3 clearly indicates that no PD-activity was present during the 10-minute measuring period for the absolute air pressure of 0.2 bar and applied test voltage of 1 kV peak. In fact, no activity was present during any of the pressure levels tested, from 1.0 to 0.2 Bars with decrements of 0.1 bar.

It should be noted that it was not possible to achieve absolute pressures lower than 0.2 bar, due to limitations of the available equipment. Conclusion of the measurement must therefore be, that no PD-activity was present for any achievable pressure level, and the transformer prototype therefore passes the ECSS requirements in all of the possible test conditions, only limited by the actual pressure vessel and vacuum pump.

An out-of-scope experiment was also conducted, where the voltage was gradually increased for the most critical pressure level, in order to experimentally determine the PD onset voltage level. The PD onset was found and measured over the same 10-minute period as the other PD-measurements and had an onset voltage at a peak voltage of 2 kV, as seen in Figure 4, and were internal PDs.

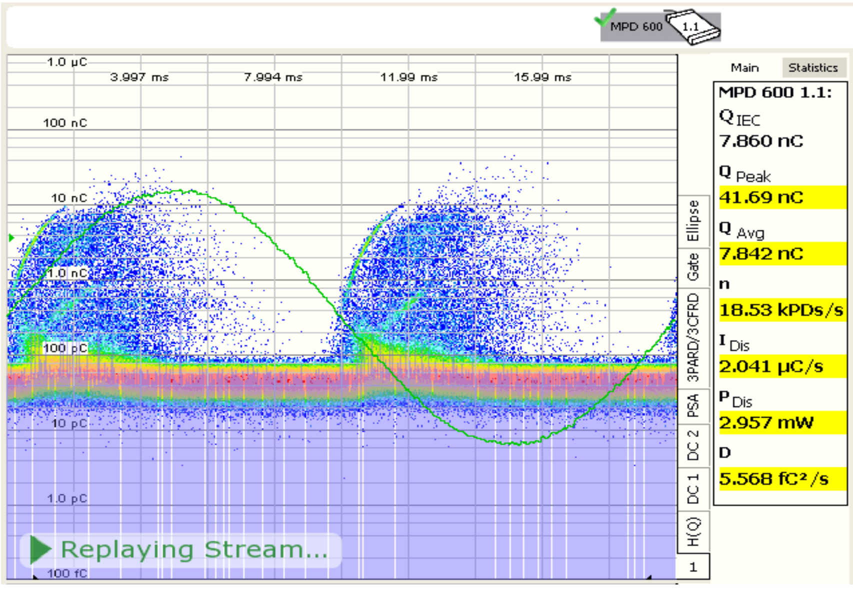

Fig. 4. PD onset at 2 kV for 0.2 bar.

Further increasing of the voltage was not done, since this would put the transformer in the risk of being destroyed – eliminating future experiments on it completely. Under a handful of the units are in existence, risking destroying one was not deemed worth it.

3 State-of-the-Art

This paper also demonstrates a strategy for evaluating corona onset based on calculation of the effective ionization coefficient along the critical electrical field line, in contrary to evaluating for corona onset purely by maximum surface electrical field strength at the critical point, adjusted to atmospheric conditions when deviating from standard conditions. The effective ionization, $\overline{\alpha}$, is given by:

$$\overline{\alpha} = \alpha - \eta \tag{1}$$

Where α is the ionization coefficient along the critical electrical field line, and η is the attachment coefficient. It should be noted that Equation (1) ceases to be valid when $\alpha \leq \eta$. The electrical field strength is simply too weak to provide a net positive ionization from this point onwards.

The ionization and attachment coefficient are calculated based on expressions developed by Sarma & Janischewskyj [4], and can be seen in Equation (2, 3):

$$\frac{\alpha}{\delta} = \begin{cases} 3632 \cdot \exp\left(-168 \cdot \frac{\delta}{E}\right) \; for \; 1.9 < \frac{E}{\delta} \leq 45.6 \\ 7385 \cdot \exp\left(-200.8 \cdot \frac{\delta}{E}\right) \; for \; 45.6 < \frac{E}{\delta} \leq 182.4 \end{cases} \quad (2)$$

$$\frac{\eta}{\delta} = 9.9865 - 0.541 \cdot 10^{-3}\left(\frac{E}{\delta}\right) + 1.118 \cdot 10^{-8}\left(\frac{E}{\delta}\right)^2 \quad (3)$$

As can be seen in Equations (2, 3), The ionization and attachment coefficients are functions of the electrical field strength E, as well as the relative air density δ. These expressions are deduced by experimental means and are empirical equations but are also valid for non-radially emitting electrical fields [4].

The effective ionization coefficient, $\bar{\alpha}$, is then integrated along the critical field line, seen in Equation (4) [5, P. 343], until the point x_c, where $\alpha - \eta = 0$, in order to determine the number of charge carriers along the critical field line:

$$\int_0^{x_c \leq d} \bar{\alpha} \, dx = \ln(N_{cr}) \quad (4)$$

For corona onset evaluation based on Equation 4, Townsend's mechanism is the governing mechanism [5, P. 325], and taking the natural logarithm on the number of charge carriers N_{cr} will equal 8 when the corona onset conditions are met.

4 FEM Model

The model-based investigation of the transformer prototype was be done by means of FEM models. The electrical field distribution can be obtained by carefully mapping the geometry of the DUT, applying a satisfactory fine mesh which has its densest areas around the conducting surfaces and applying initial and boundary conditions. Mesh density refinement was done in an iterative manner, where an initial mesh size was applied and iteratively reduced between simulations until electrical field distribution converged, meaning that additional downsizing of the mesh did not yield any meaningful improvement of results compared to the increase in computational power.

Ideally the FEM models should be three dimensional to account for the asymmetries on the transformer prototype and test environment, but the influence of the extra dimension was shown to be quite insignificant compared to the increase in the required computational power needed in such case. Pairing this with a constraint on the maximum allowed number of notes, it was deemed that the 2D models yielded a satisfactory accuracy, to be used as a rough predictive tool for corona onset evaluation in the design process of the transformer.

Several 2D FEM models were developed based on various cross-sections of the transformer, however, only the model yielding the largest electrical field strengths was chosen to be analysed, since corona would first onset from this modelled area. The cross-section yielding the largest electrical fields can be seen in Figure 5:

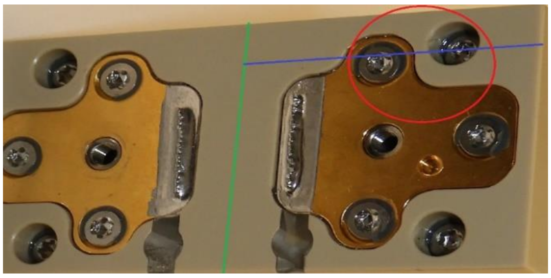

Fig. 5. Red circle: Screws investigated. Green line: Vertical symmetry axis. Blue line: Modelled cross-section.

The red circle shows two screws which possess 1 kV and ground potential respectively, since the right hand one is in galvanic contact with the grounded metal case behind the polymer. The blue line represents the cross-section which is modelled by FEM. The two brass-coloured terminals have a vertical symmetry line, which is advantageous when modelling by FEM, since the use of such line in the program can allow for more available notes.

4.1 Simulation results of the FEM model

The potential distribution, seen in Figure 6 is obtained by simulating the FEM model of the cross-section in Figure 5.

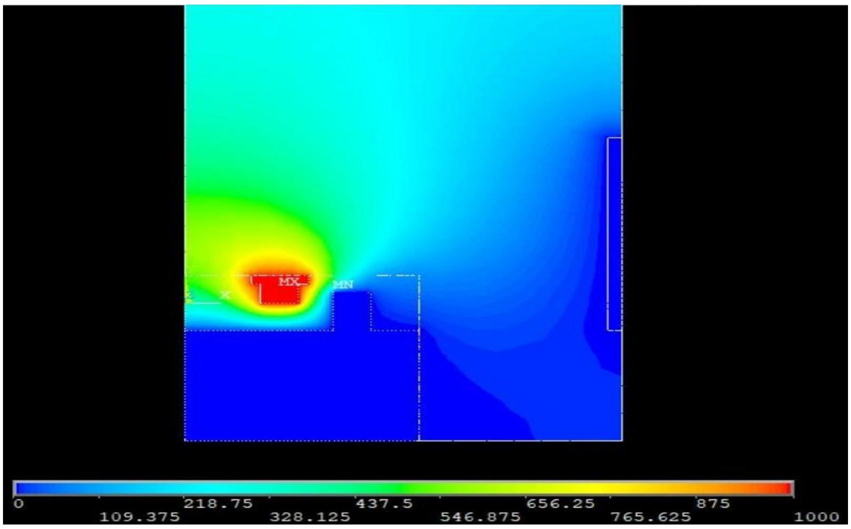

Fig. 6. Potential distribution of the modelled cross-section.

In Figure 7, the electrical field distribution was obtained by a similar approach.

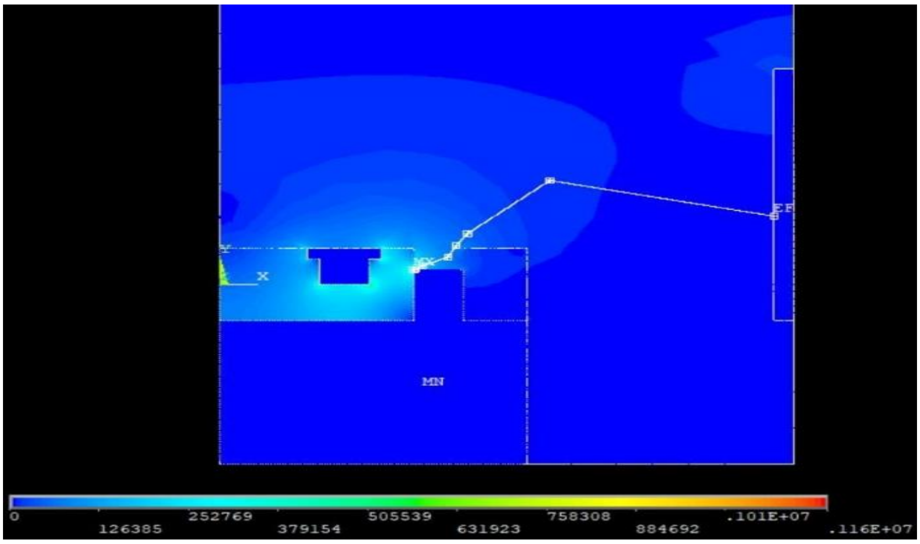

Fig. 7. Electrical field distribution and critical electrical field line of the modelled cross-section.

The critical field line originates from the point with the largest electrical field strength and propagates in such a way that it intersects the contour lines of the electrical field distribution perpendicularly and terminates on the external ground electrode mounted on the inside on the vacuum chamber. The largest electrical field strength was 11.6 kV/cm. The electrical field strength along the critical field line was then obtained and can be seen in Figure 8.

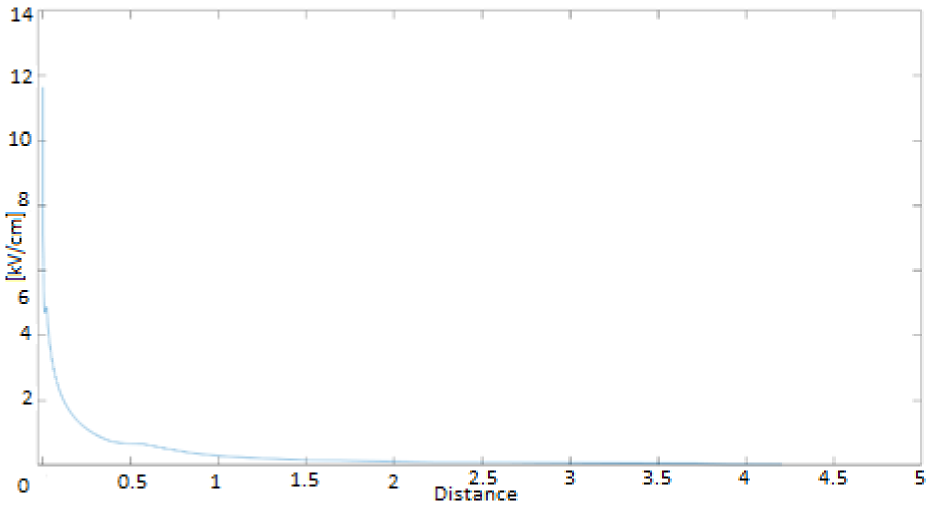

Fig. 8. Electrical field strength along the critical electrical field line.

4.2 Calculation of the Ionization and Attachment Coefficient

Calculation of the ionization and attachment coefficient along the critical electrical field line can then be done by Equation (2, 3). It should be noted that the electrical field distribution will remain constant as the geometry and applied voltage level is the same for all simulations and conducted experimental tests. Therefore, the only parameter which influences the ionization and attachment is the relative air density δ. All pressure levels used in the experimental PD-measurements were simulated for, but only the one yielding the largest effective ionization was used to evaluate the corona onset criterion. This level was an absolute pressure of 0.2 bar. The ionization and attachment coefficient along the critical line can be seen in Figure 9. The effective ionization $\overline{\alpha}$ is only defined until the intersection point, $\alpha - \eta = 0$. Therefore, the integral boundaries in Equation (4) is from zero to the point x_c where $\alpha - \eta = 0$.

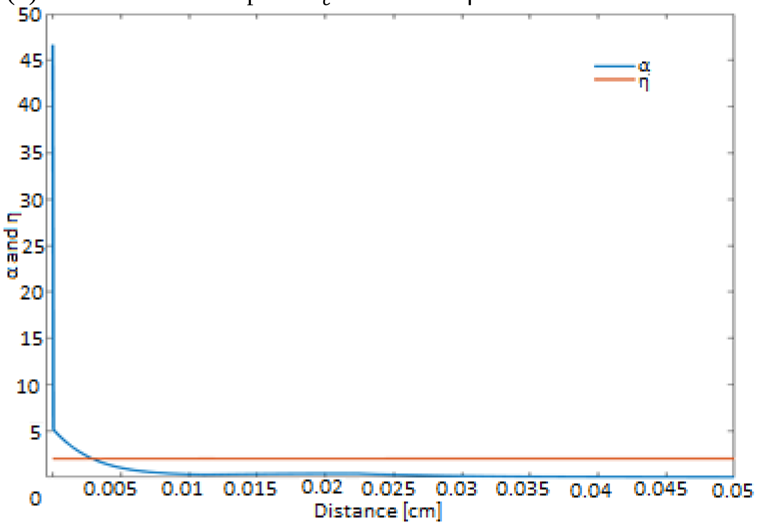

Fig. 9. Ionization and attachment coefficient along the critical electrical field line.

Evaluation of the integral in Equation (4) on obtained data in Figure 9 gives:

$$\int_0^{2.907\cdot 10^{-5}} (\alpha - \eta)dx = \ln(N_{cr}) = 0.0049 \quad (5)$$

From Equation (5) it is evident that no corona should onset for any of the pressure levels with an applied test voltage of 1 kV in the tested and modelled environment.

This simulation was repeated multiple times with varying voltage level for an absolute pressure of 0.2 bar, to find the theoretical corona onset voltage level, and this was found to be around an applied peak voltage of 3.5 kV.

5 Evaluation of Corona Onset Criterion and Ionization & Attachment Expressions

Experimental PD-measurements in Chapter 2 and FEM model results in Chapter 4.2 showed that no corona onset was happening or was expected to happen.
Modelling a coaxial cylindrical arrangement in FEM, for which well documented corona onset levels exists [5], would allow for a rough validation of validity of the corona onset criteria as well as the ionization and attachment expressions. Arbitrarily, two radii of 0.5mm and 2mm were chosen respectively for the inner and outer cylinder to be modelled. Similarly, the relative air density was chosen to be δ = 1.0.

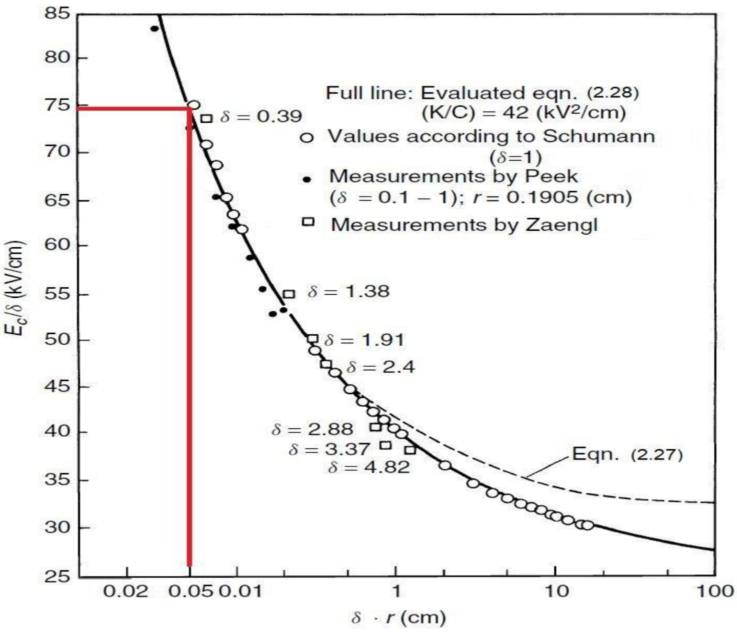

Fig. 10. Corona onset field strength as a function of the product of relative air density and radius of curvature [5].

Based on Figure 10, the corona onset field strength was determined to be 73.18 kV. This information was used to calculate the potential on the inner cylinder which yields this electrical field strength for the given radii [5]:

$$E_{max} = \frac{V}{r_1 \cdot ln(r_2/r_1)} \tag{6}$$

$$V = 73.18\frac{kV}{cm} \cdot 0.05cm \cdot ln(0.2cm/0.05cm) = 5072\,V \tag{7}$$

The coaxial cylindrical geometry was then modelled in the FEM program, and the voltage of the inner cylinder was set to 5072 V. The exact same approach as in Chapter

4.1 was then used to find the electrical field distribution as well as the critical field line, which can be seen in Figure 11:

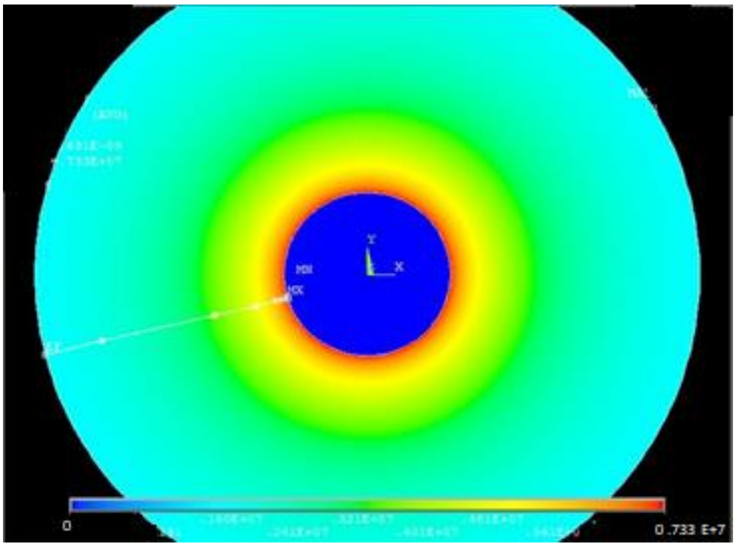

Fig. 11. Electrical field distribution of the coaxial cylindrical geometry. r1 = 0.5mm, r2 = 2mm, V = 5072 V, δ = 1.0.

The same approach as in Chapter 4.3 was applied to this model in order to determine the ionization and attachment coefficient along the critical field line, and this can be seen in Figure 12:

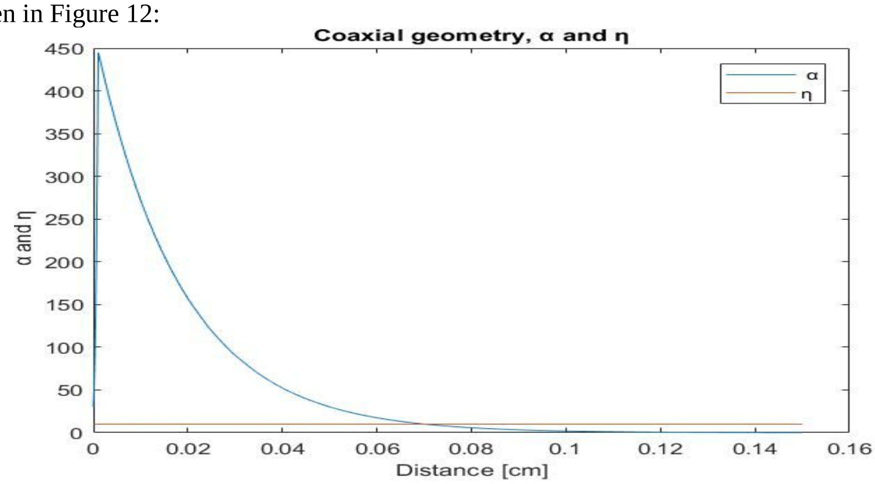

Fig. 12. Ionization and attachment coefficient along the critical field line for the coaxial cylindrical geometry.

Again, Equation (4) was evaluated to check the corona onset criterion and yielded:

$$\ln(N_{cr}) = 7.497 \qquad (8)$$

The intention of the model-based investigation was to give a rough estimate on the expectancy of corona being present for a given test case. It is concluded that the demonstrated approach in Chapter 4 can be utilized, even though the criterion is only close to being fulfilled with an integral value of 7.497 < 8. It should also be noted that the demonstration in this chapter is for a radial geometry, which is not the case for the transformer prototype.

6 Conclusions

The PD-Measurement setup was built to conform with the ECSS standard as well as the IEC 60270. The PD-measurements of the DUT showed no activity was present for the specified test cases in scope. The PD-activity onset voltage was found to be 2 kV at 0.2 bar, but of internal nature – and out of scope of this investigation. It can therefore be concluded that the design of the investigated prototype was better than the previous design with respect to PDs.

2D FEM models of the transformer were deemed to provide sufficient accuracy for the intended use of the model-based investigation. The only model presented and analysed in this paper was the one yielding the largest electrical field strengths. The analysis of this showed that no corona was to be expected during any of the PD-Measurements, which conforms with the initial experimental findings.

The work, results and methodology both in the model-based as well as the experimental based investigation of the transformer prototype provided Flux A/S state-of-the-art tools to perform similar investigations on future prototype and has influenced their design of their own PD-measurement facilities.

References

1. IEC 60270, “High-voltage test techniques – Partial discharge measurements,” (IEC 60270:2000)”, 2001.
2. OMICRON electronics GmbH (AT), “MPD 600 user Manual.” MPD600.AE.7 2013.
3. European cooperation For Space Standardization, “High voltage engineering and design handbook.” ECSS-E-HB-20-05A December 2012.
4. D. B. Phillips, R. G. Olsen and P. D. Pedrow, *“Corona Onset as a Design Optimization Criterion for High Voltage Hardware.”* IEEE Transactions on Dielectrics and Electrical Insulation (7:6), 2000. ISSN 1070-9878.
5. E. Kuffel, W.S. Zaengl and J. Kuffel. *“High Voltage Engineering Fundamentals,”* 2nd edition, 2000. ISBN 978-0-7506-3634-6.